DEEP WATER ANTIPATHARIANS: PROXIES OF ENVIRONMENTAL CHANGE[1]

Branwen Williams, Michael J. Risk, Steve W. Ross, and *Kenneth J. Sulak*

Key words: corals, nitrogen, carbon, stable isotopes, ^{210}Pb dating

ABSTRACT

Deepwater (307–697 m) antipatharian (black coral) specimens were collected from the southeastern continental slope of the United States and the north-central Gulf of Mexico. The sclerochronology of the specimens indicates that skeletal growth takes place by formation of concentric coeval layers. We used ^{210}Pb to estimate radial growth rate of two specimens, and to establish that they were several centuries old. Bands were delaminated in KOH and analyzed for carbon and nitrogen stable isotopes. Carbon values ranged from -16.4‰ to -15.7‰; the oldest specimen displayed the largest range in values. Nitrogen values ranged from 7.7‰ to 8.6‰. Two specimens from the same location and depth had similar ^{15}N signatures, indicating good reproducibility between specimens.

INTRODUCTION

Deepwater black corals (Antipatharia) have substantial potential as proxy records of historical oceanographic and biogeochemical changes (Grange and Goldberg, 1994). Their long life spans, wide geographic distribution, and large depth range (Grigg, 1965; van der Land and Opresko, 2001) suggest that they may provide environmental information in geographic locations and for periods of time not available from other sources.

The semirigid antipatharian skeleton is composed of chitin complexed with proteins (Goldberg et al., 1994). Antipatharians feed on particulate organic matter (POM) composed of detritus, marine snow, and plankton in the water column (Grigg, 1965). The transfer of POM from surface waters to the antipatharian organic skeleton indicates a link between the isotopic composition of the skeleton and surface oceanographic and biogeochemical processes affecting the constitution of POM (Heikoop et al., 1998, 2002).

Studies of growth ring structure and formation in shallow-water antipatharians suggest that the skeleton is formed of concentric coeval rings such that the inner rings of a branch are the

[1] Reproduced for this report by permission of Geological Society of America; published in: **Geology** 2006, 34:773-776.

oldest and the outside rings are the most recently formed (Grange, 1985a, 1985b; Goldberg, 1991; Grange and Goldberg, 1994). Similar growth in deepwater specimens would allow us to develop radial growth chronologies of the skeleton.

In this paper we document the sclerochronology of these deepwater corals using ^{210}Pb analysis. We test skeletal treatment with KOH to delaminate bands and analyze skeletal stable isotopic composition to obtain proxy records of environmental change.

STUDY SITES - Samples from three study sites were selected for analysis (Fig. 7.1). The Jacksonville lithoherm (Paull et al., 2000) site is at ~550–650 m depth on the Florida-Hatteras Slope ~180 km off Jacksonville, Florida. The Stetson Banks site is 380 km off Savannah, Georgia, at 650–700 m depth. Both sites are influenced by the Gulf Stream (Stetson et al., 1962; Paull et al., 2000). The third site was the Viosca Knoll area in the north-central Gulf of Mexico, ~100 km east of the Mississippi River Delta, at 300–530 m depth (Schroeder, 2002).

METHODS

SAMPLE COLLECTION - Four antipatharian specimens (Fig. 7.2) were collected (Table 1) using the Johnson Sea-Link submersible during two research cruises in 2004, 9–15 June (continental slope; southeastern U.S.) and 31 July–1 August (north-central Gulf of Mexico) (Fig. 7.1). Specimens were tentatively identified as *Leiopathes glaberrima* (Esper) (= *Antipathes glaberrima*) based on branch pattern and size, although further taxonomic validation is needed (D. Opresko, 2005, personal comm.). After collection, cenosarc was picked off with forceps. The specimens were then rinsed in seawater and air-dried on deck.

IMAGING – In the laboratory, 1-cm-thick cross sections were cut from the base of each specimen with a wafering blade attached to a Dremel Multipro drill. Polished 30 µm and 100 µm cross sections were cut adjacent to the thick sections. Digital photographs of the thin sections were taken under compound microscope with a Leica DFC300 camera to examine banding patterns. Small portions of the thick section were placed in 2 g of KOH in 50 mL of Milli-Q water for 4 h and band separation was examined using a scanning electron microscope (SEM).

SKELETAL ^{210}PB DATING - We subsampled 4-mm-thick cross sections from the bases of specimens A9902 and A8601 into three equal concentric regions labeled, from the outside to the inside, A9902-A, A9902-B, and A9902-C, and A8601-A, A8601-B, and A8601-C, respectively. Subsamples were cut with a wafering blade attached to a Dremel drill to obtain a minimum 0.5 g

of material, cleaned three times ultrasonically with Milli-Q water for 10 min to ensure removal of all particles not incorporated into the skeleton, and then dried overnight at 40°C. After cleaning, subsamples were handled with clean forceps at all times to prevent contamination. Subsamples (>0.5 g) and ^{209}Po spike (~3 dpm) were dissolved in a mixture of two-thirds concentrated HCl and one-third concentrated HNO_3 on a low-temperature hot plate until completely dissolved and dried. The dried mixture was redissolved in 0.5 N HCl; ^{210}Po was plated onto a silver disc from the solution at ~80°C for several hours. The ^{210}Po activity was counted in an Alpha Counter EGG-ORTIC 476 according to methods of Ruiz-Fernández et al. (2003).

There are three potential sources of ^{210}Pb to the antipatharian skeleton: the excess (unsupported) fraction, the supported fraction, and the in-growth fraction. The ^{210}Pb has low solubility, thus it adheres to particulate matter in the water column. The relatively slow radial growth rates of antipatharians (based on estimates from shallow-water specimens; Grange and Goldberg, 1994) provide sufficient time for particulate matter to adhere to the outside layer of the skeleton during formation; this is the source of unsupported $^{210}Pb_{ex}$ to the skeleton. The $^{210}Pb_{ex}$ fraction can be used to determine the age of a subsample; however, first the other two sources of ^{210}Pb must be accounted for. Detrital particles in the water column are also a source of supported ^{210}Pb, which comes from the decay of ^{238}U. The in-growth ^{210}Pb fraction comes from the in situ decay of ^{226}Ra taken up from seawater during skeletal formation. The supported and in-growth fractions are assumed to be 0; this is discussed in the following.

The subsamples for ^{210}Pb analysis were taken along a time-dependent growth axis from the external and youngest subsample A to the internal and oldest subsample C for both specimens. The distance from the average point of each subsample along the radial growth axis to the outside edge of the section (time = 0) was plotted against measured ^{210}Pb activity. The asymptote of the curve for specimen A9902 is essentially 0; therefore, we can assume that supported ^{210}Pb and ingrowth ^{210}Pb is 0 and thus does not need to be accounted for in this specimen. The natural log of ^{210}Pb activity for each subsample was then taken to convert the curve into a straight line in which the natural logarithm of the y-intercept represents initial activity. For specimen A9902 the trend equation is $y = -0.07563x + 1.8788$ (R^2 =0. 9993) and initial activity (A_0) = 6.84 dpm/g. This calculation assumes that initial $^{210}Pb_{ex}$ is constant in time and space.

The age of specimen A9902, based on the radioactive decay of ^{210}Pb in the coral skeleton, was calculated using: $A_{ex} = A_0 e^{-\lambda t}$ (Equation 1), where A_{ex} is the activity measured at time (t), A_0 is the initial activity at t = 0, and λ is the decay constant of ^{210}Pb (λ= 0.0311 yr^{-1}) (Druffel et al., 1990). The initial activity calculated above was then substituted into Equation 1 along with the measured excess activity to determine specimen age.

BAND SEPARATION AND ANALYSIS - A 5-mm-thick cross section from the base of each specimen was placed in a solution of 4 g of KOH in 50 mL of water for ~1 week, resulting in band delamination (Fig. 7.3). Bands were separated under a light microscope using forceps, working from the outside of the section toward the center. After removal, each band was rinsed three times in Milli-Q water and dried overnight at 40°C. Subsamples (0.7–0.8 mg) were taken from each band and analyzed for δ^{13}C and δ^{15}N. Analysis was performed on an Isoprime Mass Spectrometer in continuous flow with a Carlo Erba Elemental Analyzer. Isotopic abundances are reported in the standard delta notation versus Vienna Peedee belemnite (Coplen, 1994) and atmospheric nitrogen (Mariotti, 1984) for carbon and nitrogen, respectively, where δ^{13}C or δ^{15}N =$[(R_{sample}-R_{standard})/R_{standard}]$ [1000 ‰] and R = ^{13}C/^{12}C or ^{15}N/^{14}N. Analyses were made against internal laboratory standards and the international standards USGS-25 and IAEA C6 sucrose. Instrumental precision of the mass spectrometer is <±0.1‰ for δ^{13}C and ±0.2‰ for δ^{15}Nbased on repeated analysis of standards. Precision, and thus reproducibility, for the organic antipatharian skeleton was measured for two bands using five random replicate subsamples from each band. The combined analytical precision of both bands for δ^{13}C was ±0.04‰. For δ^{15}N, the combined precision was ±0.17‰. The effect of KOH treatment on stable isotope composition is negligible (Williams, 2005).

RESULTS AND DISCUSSION

DATING AND GROWTH RATES - These corals are long-lived and slow-growing organisms. Results and extrapolated age calculations are provided in Table 2. The ^{210}Pb activity yielded ages of 33, 95, and 163 yr for subsamples A9902-A, A9902-B, and A9902-C, respectively, and an overall age of 200 yr for a specimen with a diameter of 5.8 mm at the base. The activity of ^{210}Pb (dpm/g) for subsamples A9902-A, A9902-B, and A9902-C was 2.47 (±0.03), 0.35 (±0.01), and 0.041 (±0.004), respectively. For subsamples A8601-A, A8601-B, and A8601-C the ^{210}Pb (dpm/g) activity was 0.27 (±0.02), 0.013 (±0.005), and 0.0094 (±0.004). Specimen A9902 grew

0.97 mm in 62 yr from A9902-A to A9902-B, resulting in a growth rate of 0.015 mm yr^{-1} and 0.97 mm in 68 yr from A9902-B to A9902-C, with a growth rate of 0.014 mm yr^{-1}. The average growth rate was 0.0145 mm yr^{-1}. The average measured radius of the specimen was 2.9 mm; therefore, the total age of the specimen is 200 yr. A major assumption with this method of dating is constant growth rates. Growth-rate estimates from subsamples A9902-A to A9902-B and from A9902-B to A9902-C were very similar, suggesting that the average growth rate did not change significantly between the first and second half of the specimen's life. This assumption is supported by a comparison of growth rates between specimens A9902 and A8601. Subsample A8601-A plotted on the same line as subsamples from A9902 ($y = -0.07563x + 1.8788$) calculated from plotting the natural log of ^{210}Pb activity versus distance from the subsample center to the outside edge of the cross section. This indicated a similar growth rate between specimens. Subsamples A8601-B and A8601-C were ignored because ^{210}Pb activity was essentially zero. If average radial growth rates of deepwater *L. glaberrima* are approximately constant between specimens, this suggests by extrapolation that specimen A8601 is 480 yr, A8401 is 290 yr, and specimen AG002 is 390 yr old. Whatever the error in such extrapolation, it seems certain that each specimen is >100 yr old. Other long-lived cnidarians have been reported: the zoanthid Gerardia, formed of a layered proteinaceous skeleton, may reach ages of 1800 yr (±300 yr) (Druffel et al., 1995).

BANDING - Examination of 30 μm thin sections from all specimens under light microscope revealed banding in *L. glaberrima*, visible as banding couplets of different optical density (Fig. 7.4). The optically dark bands ranged in width from 0.002 to 0.018 mm; the optically lighter bands ranged from 0.003 to 0.022 mm. Specimen A8601 contained 460 bands, specimen A8401 contained 310, specimen A9902 contained 200, and specimen AG002 contained 230. Visual examination of thick sections polished and partially treated with KOH displayed thin layers of skeleton, 25–40 μm, tightly packed together. SEM photographs of deepwater *L. glaberrima* suggested that growth occurred by regular cyclic formation of a thin layer of skeleton. This growth pattern is similar to Gerardia, which was originally classified as an antipatharian (Druffel et al., 1995). In contrast, *A. fiordensis* grows with lighter and darker regions, and studies suggest that the optically darker bands are annual (Grange and Goldberg, 1994), the optically lighter bands being formed of cement layers (Goldberg, 1991).

The factors influencing formation of the skeletal growth layers in *L. glaberrima* are not known. Physicochemical factors potentially causing band formation in *A. fiordensis* were reviewed in Grange and Goldberg (1994); however, no correlations were found between band formation and surface or underwater light levels, salinity, or temperature. In deepwater gorgonians, variation in the structure of the skeleton may be related to food availability (Sherwood, 2002). Under nutrient rich conditions, the animal forms protein-rich organic skeleton, whereas calcite forms under nutrient-poor conditions (Sherwood, 2002). A similar mechanism could be present in the antipatharians, such that the skeleton is formed under nutrient-rich conditions, but under nutrient-poor conditions skeletal formation ceases.

STABLE ISOTOPES - Nitrogen isotope values for the specimens ranged from 7.70‰ to 8.61‰ (Table 3). The $\delta^{15}N$ signature of deepwater antipatharians is determined by their probable food source, which is believed to be falling organic matter from surface waters. The $\delta^{15}N$ specimens A8601 and A8401 were collected from comparable depths (593 and 561 m, respectively) at the Jacksonville lithoherms. They displayed similar $\delta^{15}N$ values, suggesting a similar food source, while specimen A9902, from a deeper area (679 m) and farther offshore (Fig. 7.1), is depleted in ^{15}N (7.70‰). The $\delta^{15}N$ signature of sinking particles decreases with depth (Altabet et al., 1991), which may account for the variation between specimens A8601-A8401 and A9902. Specimen AG002, from the Gulf of Mexico, was collected from the shallowest depth (307 m) and has an intermediate mean ^{15}N value (8.02‰). The $\delta^{15}N$ of organic particulate matter also reflects phytoplankton and nitrate concentration dynamics (Wada and Hattori, 1976; Altabet and Francois, 1994). The northern Gulf of Mexico receives high fluxes of nitrate fertilizer ($\delta^{15}N$ from -4‰ to 4‰; Kendall, 1998) from the Mississippi-Atchafalaya watershed (Goolsby et al., 2001). The input of ^{15}N-depleted material relative to antipatharian specimens and anthropogenic alteration of nitrogen dynamics can account for the intermediate ^{15}N value of specimen AG002 relative to the deeper Atlantic specimens.

Carbon isotope values for the four specimens ranged from -15.66‰ to -16.39‰ with a variety in range of values from 0.74‰ to 2.51‰ (Table 3). Similar to nitrogen, carbon isotopes in the skeleton likely are determined by the food source, organic matter. The average $\delta^{13}C$ value for southeastern U.S. specimens was -16.04‰ ± 0.04‰ (Table 3), although specimen A8601 from the Jacksonville lithoherms had notably lower values (-15.66‰ ± 0.05‰) than the other two southeastern U.S. specimens: A8401 (-16.31‰ ± 0.02‰) and A9902 (-16.14‰ ± 0.06‰),

and the Gulf of Mexico specimen AG002 (-16.39‰ ± 0.03‰). The $\delta^{13}C$ values for A8401 and A9902 were similar: 1.6‰ and 1.4‰, respectively, while AG002 was half as much (0.74‰) and A8601 was twice as much (2.5‰). This suggests that $\delta^{13}C_{POM}$ has been very variable over the past 500 yr in the Atlantic, possibly as a reflection of changing atmospheric carbon dioxide concentrations, and that carbon dynamics have been more stable in the Gulf of Mexico over a similar period of time.

This is the first study of possible environmental signals recorded in skeletons of antipatharians. Their wide distribution in the world's oceans, coupled with their slow growth rate, suggests that they may provide data from a range of depths on the time scale of hundreds of years.

CONCLUSIONS

Deepwater antipatharians are slow growing, with estimated radial growth rates of 0.0145 mm yr^{-1}, far slower than those recorded from warm and temperate shallow-water antipatharians. Stable isotope results are reproducible among specimens from the same location, indicating that antipatharians have potential as proxy records.

ACKNOWLEDGMENTS

This research was funded by Natural Environment Research Council grants to Risk. The National Oceanographic and Atmospheric Administration Office of Exploration provided support for this work through funding to Ross. The Gulf of Mexico cruise was supported by the U.S. Geological Survey Outer Continental Shelf Ecosystems Studies Program (Sulak). J. McKay, B. Ghaleb, A. Adamowicz, and R. Mineau helped with analyses. A. Quattrini (University of North Carolina at Wilmington) produced Figure 7.1. Specimens were identified by D. Opresko. C. Hillaire-Marcel, D. Sinclair, A. Cohen, C. Holmes, and one anonymous reviewer provided comments on the manuscript. K. Juniper generously provided laboratory space and feedback on the manuscript.

DISCLAIMER

Any use of trade, product, or firm names is for descriptive purposes only and does not imply endorsement by the U.S. Government.

LITERATURE CITED

Altabet, M., and R. Francois. 1994. Sedimentary nitrogen isotopic ratio as a recorder for surface ocean nitrate utilization: Global Biogeochemical Cycles. 8:103–116.

_____, W. Deuser, S. Honjo, and C. Seinen. 1991. Seasonal and depth related changes in the source of sinking particles in the North Atlantic: Nature. 354:136–139.

Coplen, T. 1994. Reporting of stable hydrogen, carbon, and oxygen isotopic abundances: Pure and Applied Chemistry. 66:273–276.

Druffel, E.R.M., L.L. King, R.A. Belastock, and K,O. Buesseler. 1990. Growth rate of a deep-sea coral using 210Pb and other isotopes: Geochimica et Cosmochimica Acta. 54:1493–1499.

_____, S. Griffen, A. Witter, E. Nelson, J. Southon, M. Kashgarian, and J. Vogel. 1995. Gerardia: Bristlecone pine of the deep-sea?: Geochimica et Cosmochimica Acta. 59: 5031–5036.

Goldberg, W. 1991. Chemistry and structure of skeletal growth rings in the black coral *Antipathes fiordensis* (Cnidaria, Antipatharia): Hydrobiologia. 216–217:403–409.

_____, T. Hopkins, S. Holl, J. Schaefer, K. Kramer, T. Morgan, and K. Kim. 1994. Chemical composition of the sclerotized black coral skeleton (Coelenterata: Antipatharia): A comparison of two species: Comparative Biochemistry and Physiology, 107B:633–643.

Goolsby, D., W. Battaglin, B. Aulenbach, and R. Hooper. 2001. Nitrogen input to the Gulf of Mexico: Journal of Environmental Quality. 30:329–336.

Grange, K. 1985a. Distribution, standing crop, population structure and growth rates of an unexploited resource of black coral in the southern fiords of New Zealand: Proceedings of the 5th International Coral Reef Congress, Tahiti. 6:217–221.

_____ 1985b. Distribution, standing crop, population structure, and growth rates of black coral in the southern fiords of New Zealand: New Zealand Journal of Marine and Freshwater Research. 19:467–475.

_____, and W. Goldberg. 1994. Chronology of black coral growth bands: 300 years of environmental history?, in Battershill, C., ed., Proceedings of the Second International Temperature Reef Symposium: Auckland, New Zealand, NIWA Marine Wellington, p. 169–174.

Grigg, R. 1965. Ecological studies of black coral in Hawaii: Pacific Science. 19:244–260.

Heikoop, J., M. Risk, and H. Schwarcz. 1998. Stable isotopes of C and N in tissues and skeletal organics of a deep-sea gorgonian coral from the Atlantic coast of Canada: Dietary and potential climate signals: Geological Society of America Abstracts with Programs. 30: A317, abstract 4220.

_____, D. Hickmott, M. Risk, C. Shearer, and V. Atudorei. 2002. Potential climate signals from the deep-sea gorgonian coral *Primnoa resedaeformis*: Hydrobiologia. 471:117–124.

Kendall, C. 1998. Tracing nitrogen sources and cycling in catchments, in Kendall, C., and McDonnell, J., eds., Isotope Tracers in Catchment Hydrology: Amsterdam, Elsevier Science B.V., p. 519–576.

Mariotti, A. 1984. Natural 15N abundance measurements and atmospheric nitrogen standard calibration: Nature. 311:251–252.

Paull, C., A. Neumann., B. am Ende, W. Ussler, and N. Rodriguez. 2000. Lithoherms on the Florida-Hatteras Slope: Marine Geology. 166:83–101.

Ruiz-Fernández, A., C. Hillaire-Marcel, F. Páez-Osuna, B. Ghaleb, and C. Soto-Jiménez. 2003. Historical trends of metal pollution recorded in the sediments of the Culiacan River Estuary, northwestern Mexico: Applied Geochemistry. 18:577–588.

Schroeder, W. 2002. Observations of *Lophelia pertusa* and the surficial geology at a deepwater site in the northeastern Gulf of Mexico, in Watling, L., and Risk, M., eds., Biology of cold water corals: Hyrdobiologia. 471:29–33.

Sherwood, O. 2002. The deep-sea gorgonian coral *Primnoa resedaeformis* as an oceanographic monitor [M.S. thesis]: Hamilton, Ontario, McMaster University, 65 p.

Stetson, T., D. Squires, and R. Pratt. 1962. Coral banks occurring in deep water on the Blake Plateau: American Museum Novitates. 2114:1–39.

van der Land, J., and D. Opresko. 2001. Antipatharia, in Costello, M., ed., European register of marine species: A check-list of the marine species in Europe and a bibliography of guides to their identification: Collection Patrimoines Naturels. 50:109.

Wada, E., and A. Hattori. 1976. Natural abundance of 15N in particulate organic matter in the North Pacific Ocean: Geochimica et Cosmochimica Acta. 40:249–251.

Williams, B. 2005. Deepwater antipatharian and gorgonian corals as proxies of environmental processes [M.S. thesis]: Montreal, Quebec, University of Quebec, 68 p.

ADDRESSES: (B.W.) Centre de Recherché en Géochimie et en Géodynamique, Université du Québec á Montréal-McGill, CP 8888, Succursale Centre-Ville, Montréal, Québec H3C 3P8, Canada. Current address: Department of Geological Sciences, Ohio State University, 125 South Oval Mall, Columbus, Ohio 43210. (M.J.R) McMaster University, Department of Geography and Earth Sciences, 1280 Main Street West, Hamilton, Ontario L8S4L8, Canada. (S.W.R) Centre for Marine Science, University of North Carolina at Wilmington, 5600 Marvin Moss Lane, Wilmington, North Carolina 28409, & Florida Integrated Science Center, St. Petersburg, U.S. Geological Survey, 600 Fourth Street South, St. Petersburg, Florida 33701-4846. (K.J.S) Florida Integrated Science Center, Gainesville, U.S. Geological Survey, 7920 NW 71st Street, Gainesville, Florida 32653

CORRESPONDING AUTHOR: (B.W.). E-mail: <williams.2789@osu.edu>

LIST OF TABLES

Table 7.1. Specimen collection location and diameter at base.

Specimen	Location	Lat/Long (°N/°W)	Dive #	Depth (m)	Diameter (mm)*
A8601	Jacksonville Lithoherm	30_30.1_, 79_39.2_	4684	593	14.0
A8401	Jacksonville Lithoherm	30_30.8_, 79_39.7_	4684	561	8.3
A9902	Stetson Banks	31_50.7_, 77_36.6_	4699	679	5.8
AG002	Viosca Knoll	29_06.4_, 88_23_	4744	307	11.2

*Diameter at base

Table 7.2. Subsample age and extrapolated specimen age.

Subsample	Distance (mm)	Activity (dpm/g)*	Calculated age (years) †	Extrapolated age (years) §
Specimen A9902				
A	046	2.47 (0.03)	33 (1)	
B	1.43	0.35 (0.01)	95 (2.5)	
C	2.40	0.04 (0.004)	163 (1)	
Radius	2.90		198 (2)	198
Specimen A8601				
A	1.65	0.27 (0.02)		
B	3.95	-0.01 (0.005)		
C	6.25	0.009 (0.04)		
Radius	7.00			483
Specimen A8401				
Radius	4.30			290
Specimen G002				
Radius	5.60			386

Note: Concentric, coeval subsamples were subsampled from the most recent growth (A) to the oldest growth (C). The error represents instrumental imprecision in measuring ^{210}Pb activity and the resulting calculated age.

* Activity represents $^{210}PB_{ex}$ activity.

† Calculated age determined from the decay of activity.

§ Extrapolated age based on growth rate from specimen A9902 (0.0145 mm yr^{-1}).

Table 7.3. Measured $\delta^{13}C$ and $\delta^{15}N$ isotopic abundances.

Specimen	Depth (m)	Age (years)	Mean $\delta^{13}C$ (‰)	±SE	Range (‰)	Mean $\delta^{15}N$ (‰)	±SE	Range (‰)
A8601	593	483	-15.66	0.05	2.51	8.61	0.02	3.65
A8401	561	290	-16.31	0.02	1.57	8.46	0.07	2.56
A9902	679	198	-16.14	0.06	1.42	7.70	0.15	2.56
G002	307	386	-16.39	0.03	0.74	8.02	0.19	3.36

LIST OF FIGURES

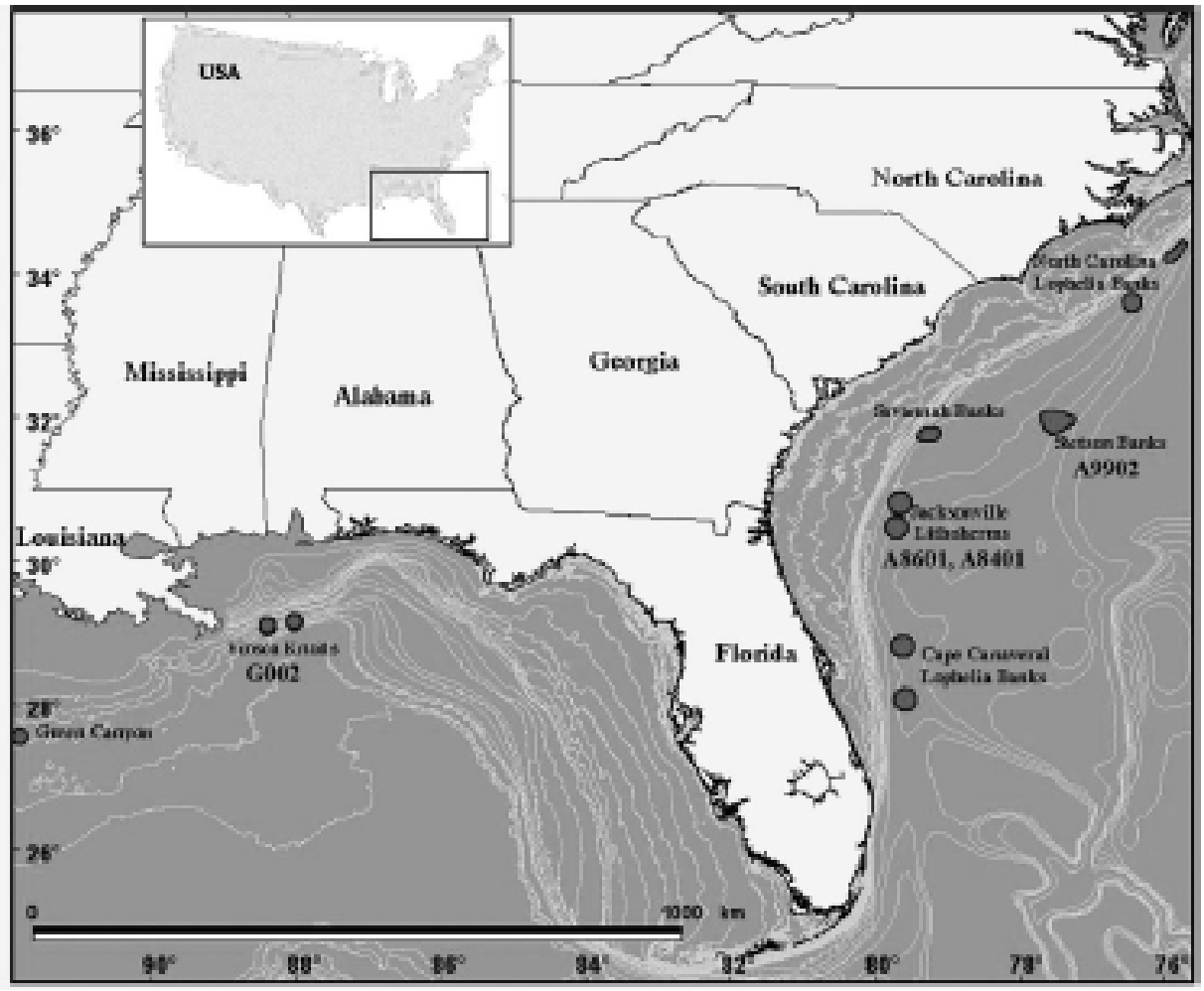

Figure 7.1. Location of antipatharian collection sites on southeastern U.S. continental slope at Jacksonville lithoherms, Stetson Bank, and Viosca Knoll.

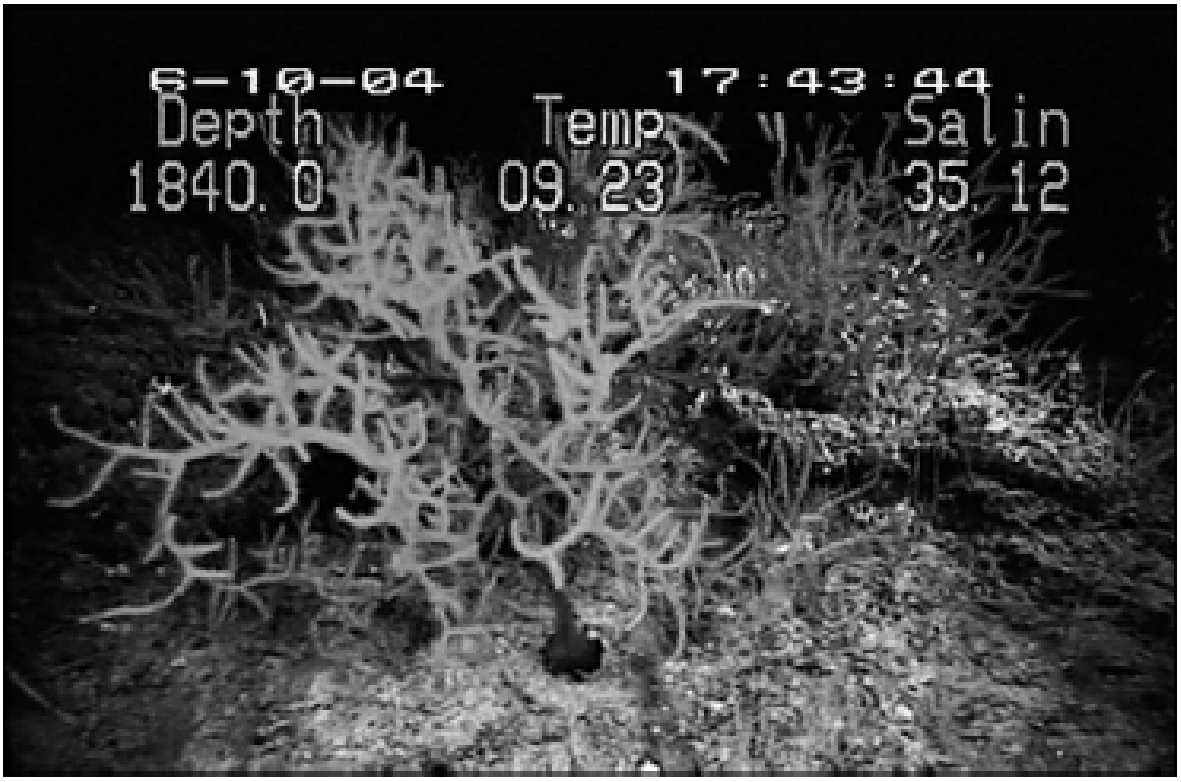

Figure 7.2. Video frame grab of black coral colony observed at 561 m at Jacksonville lithoherm site.

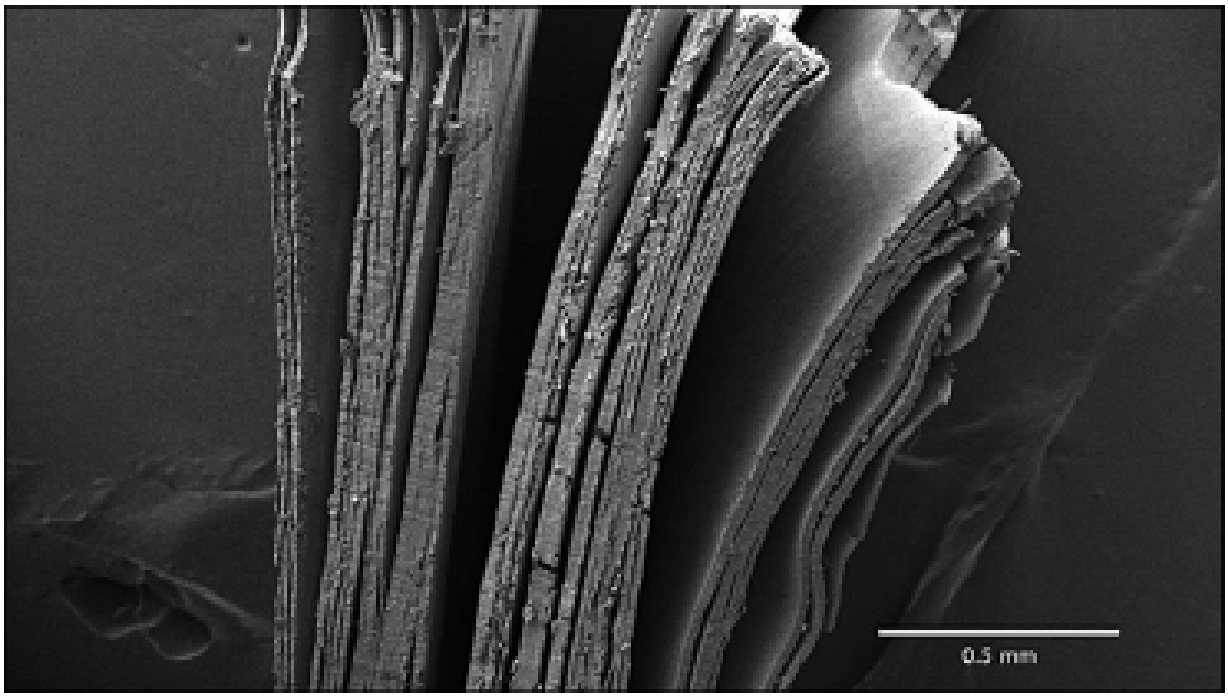

Figure 7.3. Cross-section of specimen A8601 after KOH treatment.

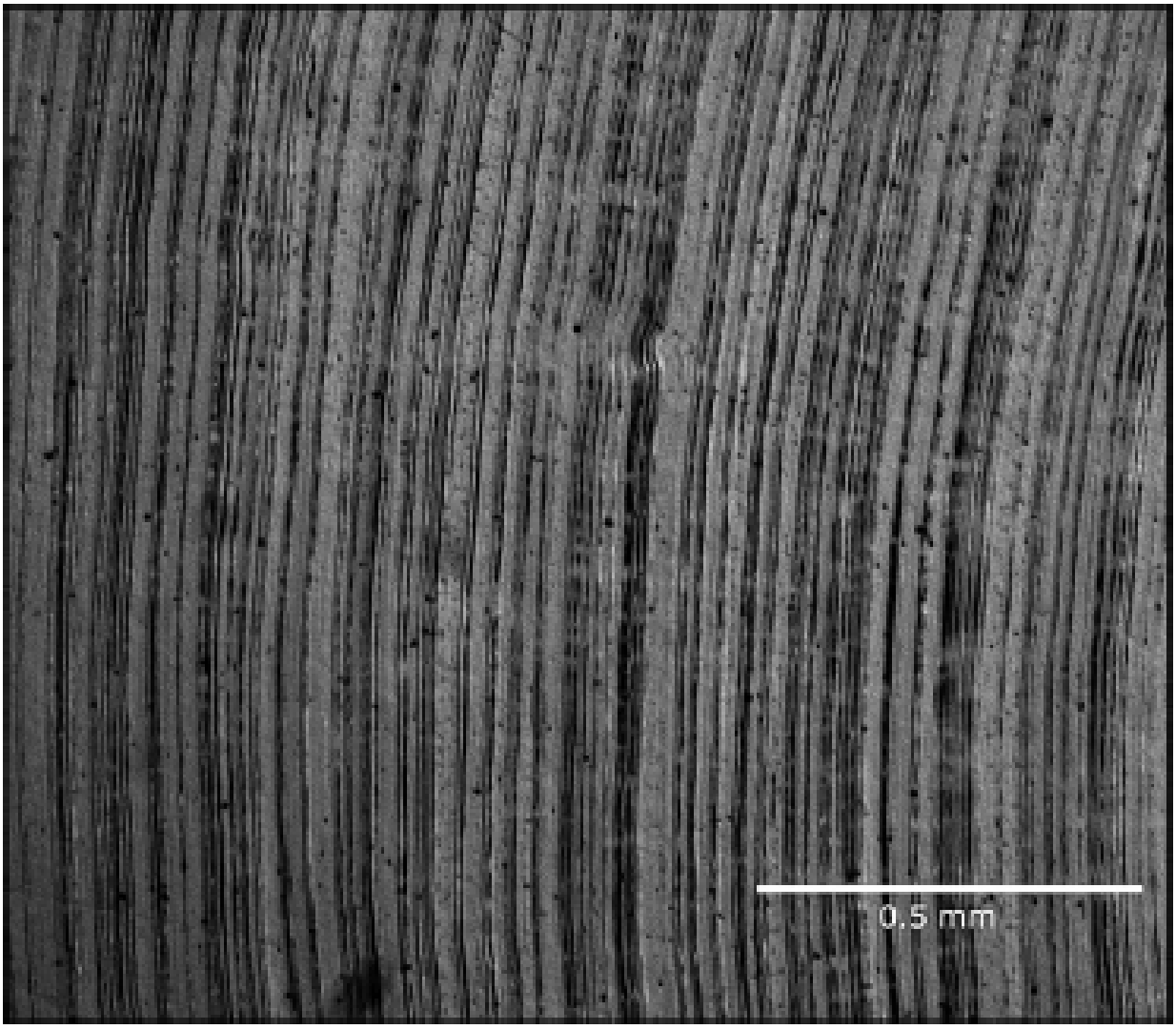

Figure 7.4. Cross-section of specimen A8601 under light microscope.